



HAL
open science

Tunnel barrier parameters and magnetoresistance in the parabolic band model

F. Montaigne, Michel Hehn, A. Schuhl

► **To cite this version:**

F. Montaigne, Michel Hehn, A. Schuhl. Tunnel barrier parameters and magnetoresistance in the parabolic band model. *Physical Review B*, 2001, 64 (14), pp.144402. 10.1103/PhysRevB.64.144402 . hal-04370640

HAL Id: hal-04370640

<https://hal.univ-lorraine.fr/hal-04370640>

Submitted on 1 Aug 2024

HAL is a multi-disciplinary open access archive for the deposit and dissemination of scientific research documents, whether they are published or not. The documents may come from teaching and research institutions in France or abroad, or from public or private research centers.

L'archive ouverte pluridisciplinaire **HAL**, est destinée au dépôt et à la diffusion de documents scientifiques de niveau recherche, publiés ou non, émanant des établissements d'enseignement et de recherche français ou étrangers, des laboratoires publics ou privés.

Tunnel barrier parameters and magnetoresistance in the parabolic band model

F. Montaigne, M. Hehn, and A. Schuhl

Laboratoire de Physique des Matériaux, UMR CNRS 7556, BP 239, 54506 Vandoeuvre lès Nancy Cedex, France

(Received 3 April 2001; published 29 August 2001)

Tunnel magnetoresistance (MR) is studied in the framework of the parabolic band model. Coherent transport and electronic wave function interferences in the barrier are shown to play an important role even for a single barrier. The influence of the barrier parameters on magnetoresistance and on its bias dependence is compared with success to experiments. The shape of the barrier is then considered as it can account for asymmetries observed in MR(V) curves. Finally, despite its simplicity, this model predicts qualitatively the complex MR(V) observed in composite barriers.

DOI: 10.1103/PhysRevB.64.144402

PACS number(s): 73.40.Gk, 73.40.Rw, 75.70.-i

Magnetoresistive tunnel junctions (MTJ) have been intensively studied in the past few years.¹ Beside the large application field of MTJ in magnetic memories, magnetic read heads or sensors and the related technological challenges, the spin-dependent tunneling effect is intrinsically a sensible probe of various physics phenomena like magnetic configurations² or interface hybridizations.³ The tunnel magnetoresistance (TMR) has been related to the spin polarization of both electrodes in the simple Jullière model.⁴ This model is the simplest expression of the more-general transfer Hamiltonian method that basically predicts tunnel currents proportional to the density of states at the electrode/barrier interfaces. This approach has been very successful to describe tunneling in superconductor tunnel junctions,⁵ but since each electrode is considered as independent, it cannot deal simply with coherent effect like quantum wells or resonant tunneling. Nevertheless, many features appearing in the magnetoresistance and in its bias dependence have been directly linked to the spin-polarized electrode band structure.^{3,6} At opposite, the free-electron-like model considers the wavefunction of electrons in the whole structure with parabolic bands. This approach has been particularly successful to describe semiconductor heterostructures like quantum wells or resonant tunneling diodes.⁷ Even if this simple band structure does not describe accurately the band structures of transition metals, this approach is well suited to study coherent effects in the tunnel current.

In this paper, we show that experimental data can be qualitatively depicted in the parabolic band-model framework using an accurate expression of the tunnel current and realistic barrier parameters. Indeed, taken into account the reduction of the effective electron mass inside the barrier, the shape of the barrier and also the tunneling of electrons with nonzero wave-vector component parallel to the tunnel barrier allow to describe the complex MR(V) experimentally observed in nonsquare or composite barriers even with a simple band structure. Those curves were up to now explained invoking exclusively the complex density of state of the electrode rather than the parameters of the tunnel barrier.

As we focus here on the influence of the barrier parameters on the properties of MTJ, the simplest band structure for the different materials, i.e., parabolic bands (free-electron-like) has been used. Furthermore, we consider parallel and antiparallel alignment of the electrode magnetiza-

tions and two-independent spin channels, with different band parameters for the ferromagnetic electrodes. Thus, following Tsu and Esaki,⁷ the tunnel current for a spin direction can be written as:

$$J = \frac{2\pi e}{h^3} m_1 \int \int D(E_z, E_{\parallel}) (f_1 - f_3) dE_z dE_{\parallel}, \quad (1)$$

where E_z (respectively E_{\parallel}) is the electron energy perpendicular (respectively parallel) to the tunnel barrier, m_1 is the electron effective mass in the emitter electrode, D is the transmission coefficient of the whole structure, deduced from the wave functions in the barrier and the electrodes, solutions of the Schrödinger equation,⁸ f_1 and f_3 are the Fermi distributions respectively in the emitter and the collector electrodes. Since most of the temperature variation of tunnel junctions characteristics at low voltages are due to the activation of inelastic modes of conduction,^{9,10} we restrict ourselves to the zero-temperature limit where expression (1) reduces to:

$$J = \frac{2\pi e}{h^3} m_1 \left(\int_0^{E_F - eV} \int_{E_F - eV - E_z}^{E_F - E_z} D(E_z, E_{\parallel}) dE_{\parallel} dE_z + \int_{E_F - eV}^{E_F} \int_0^{E_F - E_z} D(E_z, E_{\parallel}) dE_{\parallel} dE_z \right), \quad (2)$$

where E_F is the Fermi level and V the voltage applied to the collector electrode. From expression (2), it appears that the tunnel current does not depend explicitly on the density of states in the electrodes but rather on the matching of the electrodes wave functions through the barrier via the transmission coefficient D . As been stressed by Liu and Guo,⁸ a rigorous free-electron model has to “take into account the transverse (in-plane) motion of the electrons.” Indeed, refraction of the electron at the barrier interface, due to the difference of effective mass between the metal and the insulator, allows the tunneling of additional electrons. Therefore, D cannot be simply integrated over E_z but a two-dimensional integration over E_{\parallel} and E_z has to be done. This double integration is of primary importance when calculating the current through arbitrary shaped tunnel barriers as it is in the present work. In fact, in complex structures and in comparison with conventional square barriers, a nonmonotonous

evolution of D with E_z appears for lower value of E_z . This implies high-tunneling transmission of electrons with $E_{\parallel} \neq 0$. The transmission coefficient is thus integrated numerically over E_{\parallel} and E_z for each spin direction to get the total tunnel current.

Concerning the electrodes parameters, it has been shown that the tunneling current is dominated by a single free-electron-like d band in transition metals.¹¹ To model the bands of Iron, for example, parameters proposed by Stearns¹² based on Fermi surface measurements and assuming a free-electron mass are often used. Recently, Davies and MacLaren¹³ proposed for the same material other parameters fitted from first-principle band calculations [Fermi level of 2.25 eV (0.35 eV) and effective mass of $1.27 m_e$ ($1.36 m_e$) for spin up (down) band]. We will use those parameters in the following but the results presented here are essentially linked to barrier properties and do not depend much on the band structure of the electrodes. Realistic barrier parameters used in our calculations have been deduced from measurements thanks to Simmons¹⁴ fits for example. Despite it is based on the WKB approximation and thus do not describe the tunnel magnetoresistance,¹⁵ and on a constant electron mass equal to the free-electron mass in all the structure, this model provides convenient widely used analytical expressions of the tunnel current. It can be shown that fitting the $I(V)$ curves leads to an independent and good evaluation of the barrier height but does not allow the independent determination of the barrier thickness and effective mass. The latter can be measured using the variation of resistance with barrier thickness. The few-studies published^{16,17} indicate a much-lower thickness dependence than predicted using the free-electron mass. It seems thus important to consider this reduced effective electron mass in the barrier. In the following, the electron mass in the barrier was taken equal to $0.4 m_e$, the estimated value computed for crystalline alumina and in the range of values measured for SiO_2 .

This rigorous free-electron model was applied to compute the tunnel-junction current/voltage characteristics for parallel and antiparallel alignment of the electrode magnetizations as a function of barrier height and thickness. So, TMR and $V_{1/2}$, the voltage at which the magnetoresistance is divided by a factor of 2, can readily be extracted. The Fig. 1(a) represents the magnetoresistance as a function of barrier height and thickness. In the limit of null-barrier height, the situation is somehow comparable to ballistic magnetoresistance with two magnetic electrodes separated by a nonmagnetic spacer. In the limit of null-barrier thickness, very high TMR are predicted and are related to those measured in ferromagnetic ballistic nanocontacts. Outside those limits, the TMR generally increases with the barrier height and decreases with barrier thickness as observed experimentally.^{18,19} Furthermore, for realistic junction parameters, TMR decreases with the increase of the effective mass in the barrier. The predicted value of 50% for a 1 nm thick and a 3-eV high alumina barrier is in the order of reported values in the literature. In agreement with Lu *et al.*²⁰ who have experimentally shown that $V_{1/2}$ is almost independent on the electrode materials, barrier height, thick-

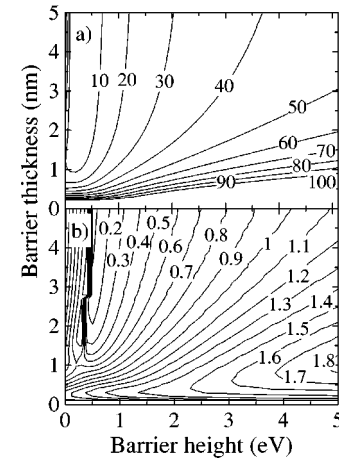


FIG. 1. (a) Magnetoresistance and (b) $V_{1/2}$ as a function of the barrier height and thickness. The effective mass in the barrier is taken equal to $0.4 m_e$. Magnetoresistances above 100% are not represented.

ness, and effective mass seem to be the main parameters governing the value of $V_{1/2}$. As it was pointed out by the experiments¹⁹ and verified with our calculations, the increase of $V_{1/2}$ with the decrease of barrier thickness or increase of barrier height appears also as an intrinsic properties. $V_{1/2}$ is drastically increased by the reduction of the effective mass and the calculated values for $m_2 = 0.4 m_e$ are superior to the experimental values [Fig. 1(b)]. Nevertheless, we only consider here coherent elastic transport but it is also well known that voltage-excited magnons are a source of spin flip and contribute to the reduction of $V_{1/2}$.⁹ This also explains the discrepancy between experimental and calculated MR(V) curves at low voltages (Fig. 2).

The decrease of the magnetoresistance with the applied voltage is almost independent of the parameters of the electrode-parabolic band structure. For applied voltages above the barrier height, oscillations of magnetoresistance are predicted and are not much affected by the band structures of the electrodes (from Stearns¹² or Davies and MacLaren¹³). In contrast, their period decreases for increased thickness or effective mass m_2 of the barrier but increases

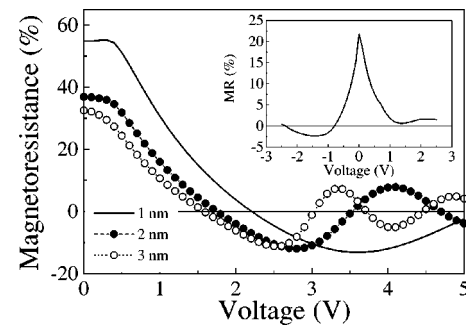


FIG. 2. Variation of magnetoresistance with applied voltage for a 1 nm (-), 2 nm (-●-), and 3-nm (-○-) thick tunnel barrier. In those calculations, $m_2 = 0.4 m_e$ and the barrier height is equal to 2 eV. Inset: experimental data of magnetoresistance with applied voltage from Ref. 21 for a $\text{Co}/\text{Al}_2\text{O}_3/\text{Co}$ junction.

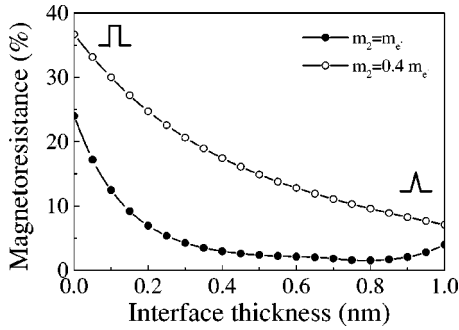


FIG. 3. Variation of magnetoresistance with interface thickness for $m_2=0.4 m_e$ ($-\circ-$) and $m_2=m_e$ ($-\bullet-$).

with the barrier height. The oscillations of magnetoresistance observed experimentally (inset of Fig. 2) can thus be interpreted in term of interferences of the wave functions in the conduction band of the insulator. This effect is totally similar to the conductance oscillations observed in the Fowler-Nordheim regime. Negative TMR for applied voltage equal or above the barrier height appears as a “standard” effect but like every coherent effect, these oscillations can be affected or suppressed by the scattering. In conclusion, the parabolic band model reproduces qualitatively the experimental measurements made on MTJ.

Recently, Zhang and Levy¹⁵ raised a restriction to this model: “the sensitivity of the magnetoresistance to the details of the profile of the potential barrier between the metallic electrodes and the insulating barrier.” Our calculations have thus been extended to MTJ with an imperfect interface between the metal and the insulator. We chose trapezoidal barriers for which the potential varies linearly in an interface region between the metal and the square barrier (Fig. 3). As predicted by Zhang and Levy, the magnetoresistance is strongly suppressed by an interfacial region when considering a free-electron mass in the barrier. But for a reduced electron-effective mass, the sensitivity is decreased and high TMR can be achieved even for mixed interfaces. Then a more abrupt interface sharpness, compatible with a more uniform oxygen concentration in the barrier after temperature annealing, is at the origin of a TMR increase by a factor of 2 as showed by Sousa *et al.*¹⁸

This analysis can be further extended to barriers with two different interface sharpness. Figure 4 represents MR(V) curves for a square ($-$), a symmetric trapezoidal ($-\circ-$), and a nonsymmetric with one abrupt interface ($-\bullet-$) barriers. Voltage dependence of the magnetoresistance is enhanced for the trapezoidal barrier and is highly asymmetric for the asymmetric interfaces. In this last case, for a positive-applied voltage, i.e., electrons collected in the electrode with the nonabrupt interface, the voltage dependence is similar to the one computed for the symmetric trapezoidal barrier. Inversely, for negative voltage, it is similar to the square barrier. Finally, the voltage dependence of the MR is strongly ruled by the interface collecting the transmitted electrons. This fact is illustrated in the inset of Fig. 4 for different Ta-oxide barriers obtained from the oxidation of a deposited Ta layer [data from Ref. 19, and same effects are observed for alumina barriers²¹]. While the sharpness of the Ta-layer

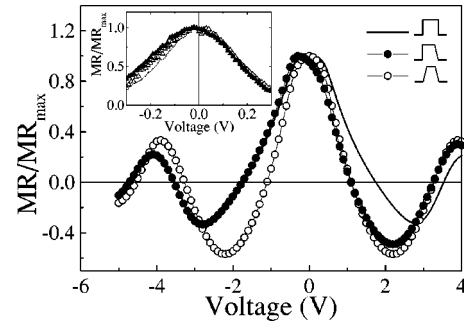


FIG. 4. Variation of magnetoresistance normalized to its maximum value with applied voltage and different barrier shapes : two ($-$), one ($-\bullet-$), and zero ($-\circ-$) sharp interface(s). In those calculations, $m_2=0.4 m_e$, the total barrier thickness is 2 nm and the thickness of the interfaces is 0.2 nm. Inset: experimental data of magnetoresistance normalized to its maximum value with applied voltage from Ref. 19 for a Co/TaOx/Co junction.

interface exposed to the oxygen plasma remains unchanged, the one of the buried interface depends on the oxidation conditions and Ta-layer thickness.

The diversity of insulators used recently to make MTJ opens the way towards composite barriers made using two insulators with different barrier heights. In Fig. 5, the voltage dependence of the TMR is represented for a composite barrier formed by 1 nm of low-barrier height insulator (0.3 eV) and 1 nm of high-barrier height insulator (2 eV). The striking feature is the inversion of TMR at low voltages and the important negative TMR. It has been indeed observed experimentally by Sharma *et al.* in $\text{Al}_2\text{O}_3/\text{Ta}_2\text{O}_5$ composite barriers⁶ and has been attributed to the electrode band structure. The voltage dependence of the effect can be reproduced considering a lower-barrier height for Ta oxide than for Al_2O_3 (Fig. 5) as already measured.¹⁹ The I(V) characteristics (not represented) of such structures present important asymmetries that can reach a factor of 10 in the current for voltages of about 1 V. The current asymmetry increases with the thickness of the low-barrier height. This asymmetry predicted for this type of barrier is very promising for magnetic random access memory applications.

To conclude, we showed in this paper that despite its sim-

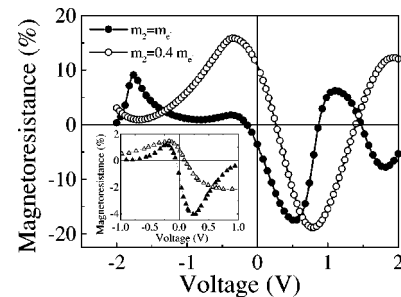


FIG. 5. Variation of magnetoresistance with applied voltage with $m_2=0.4 m_e$ ($-\circ-$) and $m_2=m_e$ ($-\bullet-$) for a composite barrier formed by a 1-nm thick low-barrier height insulator (0.3 eV) and a 1-nm thick high-barrier height insulator (2 eV). Inset: experimental data of magnetoresistance with applied voltage for a composite $\text{Al}_2\text{O}_3/\text{Ta}_2\text{O}_5$ barrier from Ref. 6.

plicity, a free-electron-like model reproduces well main features of magnetic tunnel junctions characteristics. Particularly, it reflects qualitatively the $I(V)$ characteristics, the decrease of the magnetoresistance with the voltage, the oscillations of magnetoresistance at high voltages, the important effect of a nonuniform barrier and the influence of the interfaces. This simple model cannot render all the complexity of magnetic-tunnel junctions related to complex band structures, nonideal interfaces and thus nonconservation of k_{\parallel} , elastic and inelastic scattering. But this approach considering the whole structure and the interferences of the electron

wave function leads to complex behavior of the magnetoresistance as a function of the voltage with negative and positive magnetoresistance even for simple parabolic bands. It thus may be important to consider these effects before ascribe directly $MR(V)$ curves to the density of states of electrodes, especially for composite barriers with different barrier heights.

The authors thank P. Rottländer and C. Tiusan for valuable discussions. This work was partly supported by the EC - IST program "NanoMEM" No. IST-1999-13471.

-
- ¹J.S. Moodera, L.R. Kinder, T.M. Wong, and R. Meservey, *Phys. Rev. Lett.* **74**, 3273 (1995).
- ²M. Hehn, O. Lenoble, D. Lacour, C. Féry, M. Piécuch, C. Tiusan, and K. Ounadjela, *Phys. Rev. B* **61**, 11 643 (2000).
- ³J.M. De Teresa, A. Barthélémy, A. Fert, J.P. Contour, R. Lyonnet, F. Montaigne, P. Seneor, and A. Vaures, *Phys. Rev. Lett.* **82**, 4288 (1999).
- ⁴M. Jullière, *Phys. Lett.* **54A**, 225 (1975).
- ⁵I. Giaver, *Phys. Rev. Lett.* **5**, 464 (1960).
- ⁶M. Sharma, S.X. Wang, and J.H. Nickel, *Phys. Rev. Lett.* **82**, 616 (1999).
- ⁷R. Tsu and L. Esaki, *Appl. Phys. Lett.* **22**, 562 (1973).
- ⁸S.S. Liu and G.Y. Guo, *J. Magn. Magn. Mater.* **209**, 135 (2000).
- ⁹S. Zhang, P.M. Levy, A.C. Marley, and S.S.P. Parkin, *Phys. Rev. Lett.* **79**, 3744 (1997).
- ¹⁰C.H. Shang, J. Nowak, R. Jansen, and J.S. Moodera, *Phys. Rev. B* **58**, R2917 (1998).
- ¹¹W.H. Butler, X.-G. Zhang, T.C. Schulthess, D.M.C. Nicholson, A.B. Oparin, and J.M. MacLaren, *J. Appl. Phys.* **85**, 5834 (1999).
- ¹²M.B. Stearns, *J. Magn. Magn. Mater.* **5**, 167 (1977).
- ¹³A.H. Davies and J.M. MacLaren, *J. Appl. Phys.* **87**, 5224 (2000).
- ¹⁴J.G. Simmons, *J. Appl. Phys.* **34**, 1793 (1963).
- ¹⁵S. Zhang and P.M. Levy, *Eur. Phys. J. B* **10**, 599 (1999).
- ¹⁶M. Covington, J. Nowak, and D. Song, *Appl. Phys. Lett.* **76**, 3965 (2000).
- ¹⁷H. Boeve, J. de Boeck, and G. Borghs, *J. Appl. Phys.* **89**, 482 (2001).
- ¹⁸R.C. Sousa, J.J. Sun, V. Soares, P.P. Freitas, A. Kling, M.F. da Silva, and J.C. Soares, *J. Appl. Phys.* **85**, 5258 (1999).
- ¹⁹P. Rottländer, M. Hehn, O. Lenoble, and A. Schuhl, *Appl. Phys. Lett.* **78**, 3274 (2001).
- ²⁰Y. Lu, X.W. Li, Gang Xiao, R.A. Altman, W.J. Gallagher, A. Marley, K. Roche, and S. Parkin, *J. Appl. Phys.* **83**, 6515 (1998).
- ²¹F. Montaigne, Ph.D. thesis, Université de Paris-VII, 1999.